



LAWRENCE  
LIVERMORE  
NATIONAL  
LABORATORY

# In vivo testing of a prototype system providing simultaneous white light and near infrared autofluorescence image acquisition for detection of bladder cancer

S. G. Demos, M. C. Jacobson, R. D. White

July 11, 2011

Journal of Biomedical Optics

## **Disclaimer**

---

This document was prepared as an account of work sponsored by an agency of the United States government. Neither the United States government nor Lawrence Livermore National Security, LLC, nor any of their employees makes any warranty, expressed or implied, or assumes any legal liability or responsibility for the accuracy, completeness, or usefulness of any information, apparatus, product, or process disclosed, or represents that its use would not infringe privately owned rights. Reference herein to any specific commercial product, process, or service by trade name, trademark, manufacturer, or otherwise does not necessarily constitute or imply its endorsement, recommendation, or favoring by the United States government or Lawrence Livermore National Security, LLC. The views and opinions of authors expressed herein do not necessarily state or reflect those of the United States government or Lawrence Livermore National Security, LLC, and shall not be used for advertising or product endorsement purposes.

# **In vivo testing of a prototype system providing simultaneous white light and near infrared autofluorescence image acquisition for detection of bladder cancer**

**Michael C Jacobson, Ralph deVere White**  
UC Davis Medical Center

**Stavros G. Demos,**  
Lawrence Livermore National Laboratory

## *Abstract*

A prototype instrument developed to provide simultaneously ordinary visual endoscopy together with NIR autofluorescence imaging via parallel image acquisition is demonstrated. The two images are recorded concurrently, and the instrument interfaces with any ordinary endoscope. Preliminary results of a pilot study focused on imaging of bladder tumors in vivo using this instrumentation are presented. The experimental results demonstrate the capabilities of this instrumentation design, imaging methodology and define the current limitation for further development of the system.

### *Introduction*

Cancer detection and treatment in hollow organs (e.g. GI tract, airways, urinary tract, uterus) depends heavily on endoscopic techniques that conventionally utilize white light to illuminate, visually inspect the space of interest, and guide biopsy and excision of suspicious lesions. A major theme driving current endoscopic research is that while visual detection of raised tumors within these spaces is straightforward, malignant and pre-malignant lesions that are flat or small may appear macroscopically similar to inflamed, or even normal tissues. This limitation may hinder early detection of aggressive cancers, often leaving collection of random and repeat biopsies as the only viable strategy available for surveillance in high risk patients. In an effort to address these problems, several optical methods have been investigated as a tool to complement white light endoscopy for more accurate and complete treatment of diseased tissues. These include microscopic imaging techniques (e.g. optical coherence tomography—OCT, endo-cytoscopy, and confocal fluorescence microscopy), light scattering (e.g. Raman spectroscopy), and fluorescence imaging techniques which involve the excitation and detection of either native tissue fluorophores (autofluorescence), or the use of exogenous fluorescent materials and precursors [1, 2].

From a clinician's point of view, the ideal optical adjunct for endoscopic procedures would increase the sensitivity and specificity of detecting malignant and pre-malignant lesions, reliably identify the lateral and deep margins required for complete resection, detect residual tumor within a previous resection bed, adapt easily to work with existing endoscopic technology, not require the use of toxic or inconvenient chemicals or pharmaceuticals, and allow simultaneous display of a conventional white light image such that endoscopic surgery could be guided by the technique in real time. Fluorescence

based imaging techniques in particular have shown promise in being able to deliver on many of these endoscopic requirements, and are already in routine use in a number of clinical applications including visible autofluorescence imaging in GI endoscopy[3] and bronchoscopy [4, 5].

Autofluorescence (AF) signal in the visible part of the spectrum tends to be higher in normal tissue than in cancer. Lesion identification relies, therefore, on detection of a decrease in fluorescence compared to normal tissue[2]. The most important endogenous fluorophores in the visible wavelengths are present in high concentrations in connective tissue as a result of amino acid crosslinking (collagen, elastin), and in certain molecules associated with cellular metabolism such as the reduced form of nicotinamide adenine dinucleotide (NADH) and flavins[6]. In the near-infrared (NIR) part of the spectrum, the most important endogenous fluorophores are thought to be porphyrins[7] which tend to be more highly concentrated in malignant than benign tissue[8] and are able to be excited by visible light with relatively long wavelengths compared to molecules that emit visible fluorescence. Our group has previously demonstrated that several types of malignant tumors can be differentiated *in vitro* from contiguous normal tissue by inducing excitation under long-wavelength laser illumination and imaging the resulting autofluorescence in the near infrared (NIR)[9, 10] The potential advantages of using longer excitation wavelengths are greater tissue penetration depth of the probe light and reduced artifacts arising from non-uniform concentration of blood which is a very strong absorber of the visible light. In addition, by appropriate separation of the visible white light and NIR autofluorescence (NIR AF) image components, simultaneous collection of both images is possible using conventional endoscope designs with each image acquired

at a different frame rate as needed without imposing any limitation on the acquisition of the complementary image component.

In this paper we describe a prototype instrument that we developed to simultaneously conduct ordinary visual endoscopy together with NIR autofluorescence imaging via parallel image acquisition. The two images are recorded concurrently, without the need to switch back and forth between imaging modes, and the instrument interfaces with an ordinary endoscope. For our initial investigation using this instrument, we conducted an *in vivo* pilot study of bladder tumors to build on our previous work with NIR autofluorescence of bladder cancer using *ex vivo* specimens and define the current limitation for further development of the system.

### *Materials and Methods*

Figure 1 shows a schematic representation of the prototype NIR autofluorescence endoscopy instrument. The system utilizes a standard cystoscope lens (ACMI) and the accompanying illumination fiber but the illumination source and imaging systems are modified. Specifically, the input side of cystoscope's light guide (which transports the external white to the light pillar of the cystoscope) is attached to a specially made illumination assembly designed to provide a) monochromatic laser illumination at 650 nm and b) visible white light with all spectral components above 650 nm removed. The white light is obtained from a xenon endoscopy light source (Stryker) and is transported to the illumination assembly with a 4 mm diameter liquid light guide (Edmund optics). The output of the light guide is collected and refocused in to the input of the cystoscope's light guide using a system of lenses after passing through three (3) 650 nm short-pass

interference filters to allow only transmission of photons in the visible light spectrum. This light was combined with the output of a CW laser operating at 650 nm (PLT Technology, Model 650-4-F) which was transported into the illumination assembly with a fiber after passing through a 650 nm narrow-band filter to ensure monochromatic illumination. This provides a combined visible white light and 650 nm laser light in to the tissue target location. The output power at the tip of the cystoscope is about 220 mW of visible light and about 150 mW of 650 nm laser light.

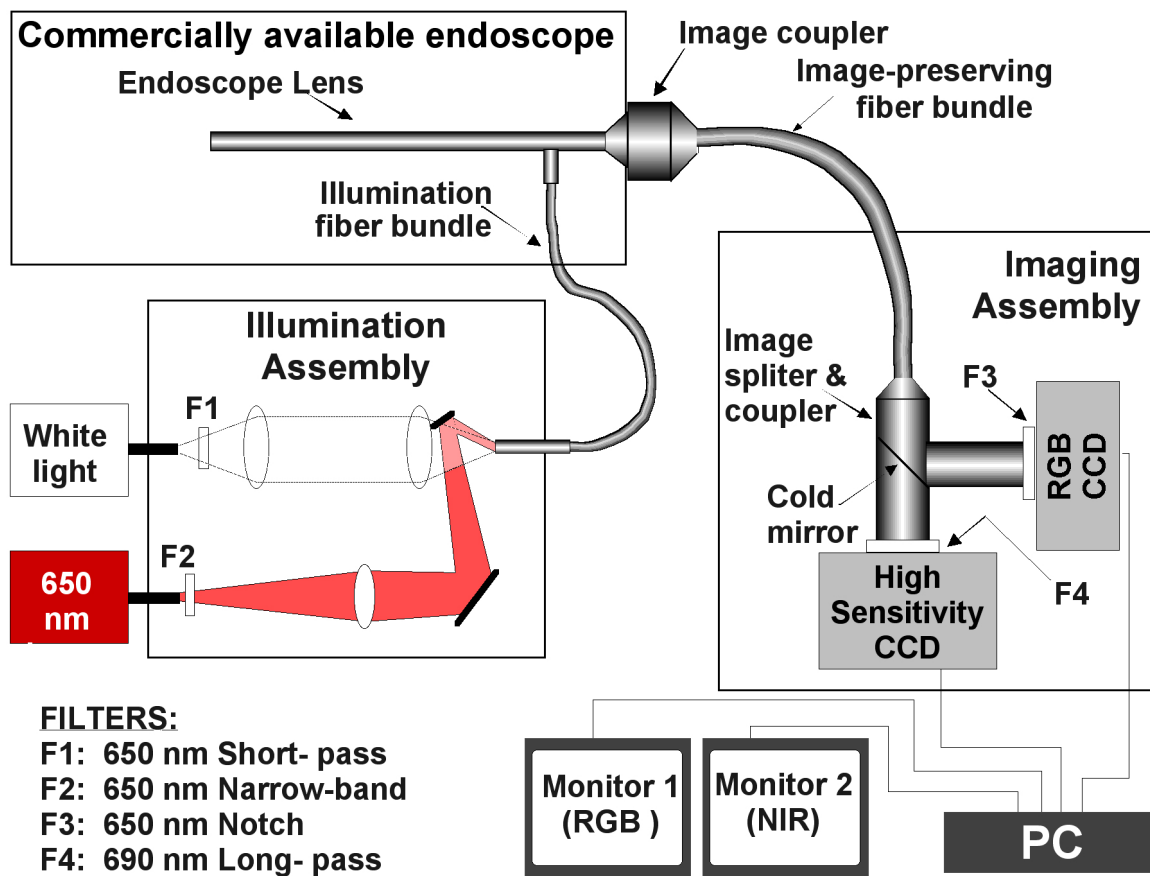


Figure 1: Schematic diagram depicting the main optical components of the prototype imaging system providing simultaneous acquisition of visible light scattering and NIR autofluorescence images.

The resultant images at the output of the cystoscope lens are coupled in to an image-preserving fiber optic bundle (SCHOTT North America, Inc.) using a standard  $f=25$ -mm C-mount endoscopy video coupler (Western Photonics Technology). This image preserving fiber bundle has a 4 mm X 4 mm square field of view and a length of 268 cm . The overall transmission of the image preserving fiber bundle in the visible and NIR spectral region is on the order of 40% while the individual fibers are 10  $\mu$ m in diameter (8  $\mu$ m core diameter). The image preserving fiber provides a reliable way to avoid achromatic aberrations of the two transmitted image components, (the visible light scattering image and the NIR AF image). In this arrangement, the two image components are transported into the imaging assembly where they are split using a system of lenses and a cold mirror which reflect the visible image component and transmit the NIR image component. The NIR image is passed through a 690 nm long-pass filter before being projected onto a high sensitivity 512X512 pixel, air cooled Charge Couple Device (CCD) camera (Princeton Instruments, Cascade). The visible image reflected by the cold mirror is passed through a 650 nm notch filter to remove any scattered light from the laser. It is then collected by a digital red-green-blue (RGB) CCD. The signals from both CCDs are separately processed by a personal computer and displayed simultaneously on two separate monitors. AVT Smartview software (Allied Visiontec) was used to process and display of RGB images (15 frames/second) and an image was saved every 15<sup>th</sup> frame (1 image per second). Winview/32 (Princeton Instruments) was used to process and display the NIR AF images with exposure time of 500 msec and saved on the computer. The instrumentation discussed above was assembled in to a portable system that was easily transportable into the operating room.

This 4-level portable system contained the light sources and power supplies at the lower level, the illumination and imaging assemblies in the middle sections, while the computer and monitors were positioned at the top for easy access and visibility.

We conducted preliminary testing of the system's ability to acquire NIR AF images while simultaneously displaying the conventional color (RGB) image in 21 patients undergoing transurethral resection of bladder tumors at UC Davis Medical Center. These experiments were approved by the UC Davis institutional review board. After the tumor and the region of interest were initially defined via standard video cystoscopy, the standard coupler and video camera enabling the conventional RGB imaging were detached from the cystoscope and were replaced by the coupler and image preserving fiber bundle of the prototype system. The input of the cystoscope's light guide was detached from the conventional light source and coupled to the illumination assembly of the prototype system. The system was then used to capture RGB and NIR AF images of the region of interest while these images were displayed in separate adjacent monitors which guided the operator. The entire process of connecting the prototype system to the cystoscope, acquiring the in vivo data and, reverting to the regular RGB camera was accomplished within a time window of about 2 minutes. These measurements were performed both before and after tumor resection. Data were also recorded for each patient's tumor size, grade, and depth of invasion based on subsequent pathology report.

For each patient, the RGB images were used to manually map the location of apparently normal tissue and tumor tissue on the corresponding NIR images. Upon selection of the area of interest in the RGB image, the corresponding NIR image was

identified by a time tag. Because of the difficulty in normalizing excitation intensity with the current setup, we did not attempt to quantify the signal in the current set of experiments.

Ultimately we had four specific goals for this set of experiments: 1. To demonstrate that simultaneous acquisition of standard video cystoscopy RGB images and NIR autofluorescence image is possible using the prototype system. 2. To show that blood does not cause a large artifact with this method. 3. To confirm that the findings from the previous study performed on *ex vivo* specimens could be reproduced *in vivo*. 4. To determine the limitations of the method and plan future improvements of the technique.

Demonstration of the type of images obtained using this system is shown in Figure 2. This image was obtained *in vivo* from a normal bladder tissue area exhibiting normal vascularity. The image on the left side is the white light RGB image and the image on the right side is the NIR AF image that was simultaneously acquired. The latter image is smooth showing no features that could correlate to the location of blood concentration shown in the corresponding RGB image. This also provides an example of our findings for goal #2 listed above (i.e. showing whether the presence of blood would affect the image quality of the autofluorescence image). Moderate amounts of blood do not give rise to corresponding image artifacts in the NIR AF images.

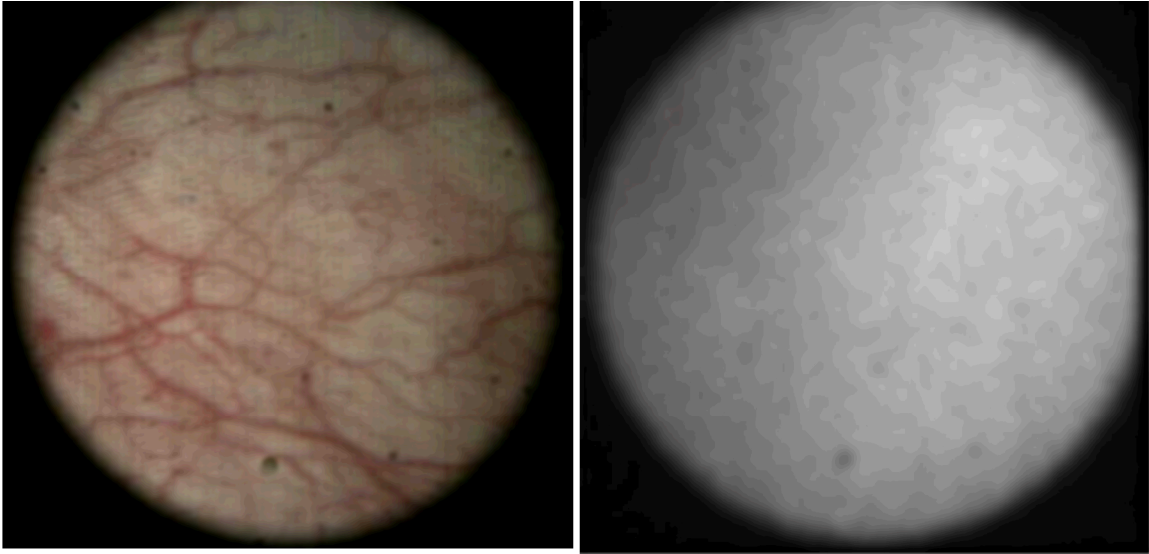


Figure 2: RGB and corresponding NIR images of a normal tissue area with well defined vasculature.

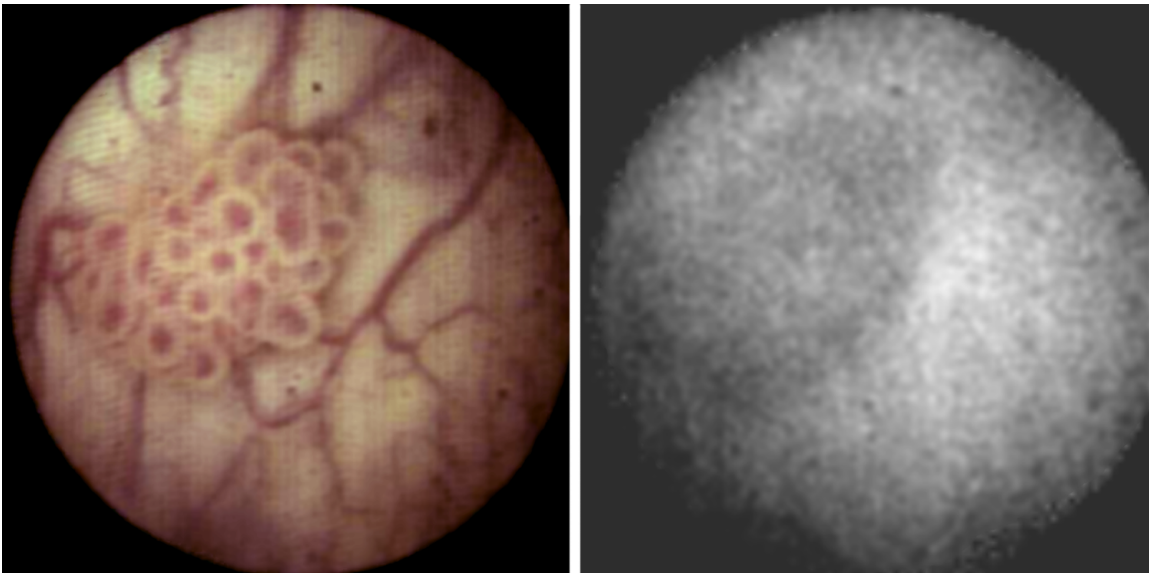


Figure 3: RGB and NIR images of a 1 cm papillary bladder tumor; Ta high grade urothelial carcinoma.

Figure 3 shows that RGB and corresponding NIR AF image from the location of a tumor. The polypoid tumor is clearly visible in the RGB image but it only appears as a dark object in the NIR AF image. This is in agreement with the ex vivo study where the tumors were detected with lower intensity compared to normal bladder tissue. Pathology

classified this tumor as High Grade Ta, indicating the superficial and non-invasiveness of the lesion but with cellular features that are consistent with a relatively aggressive cancer.

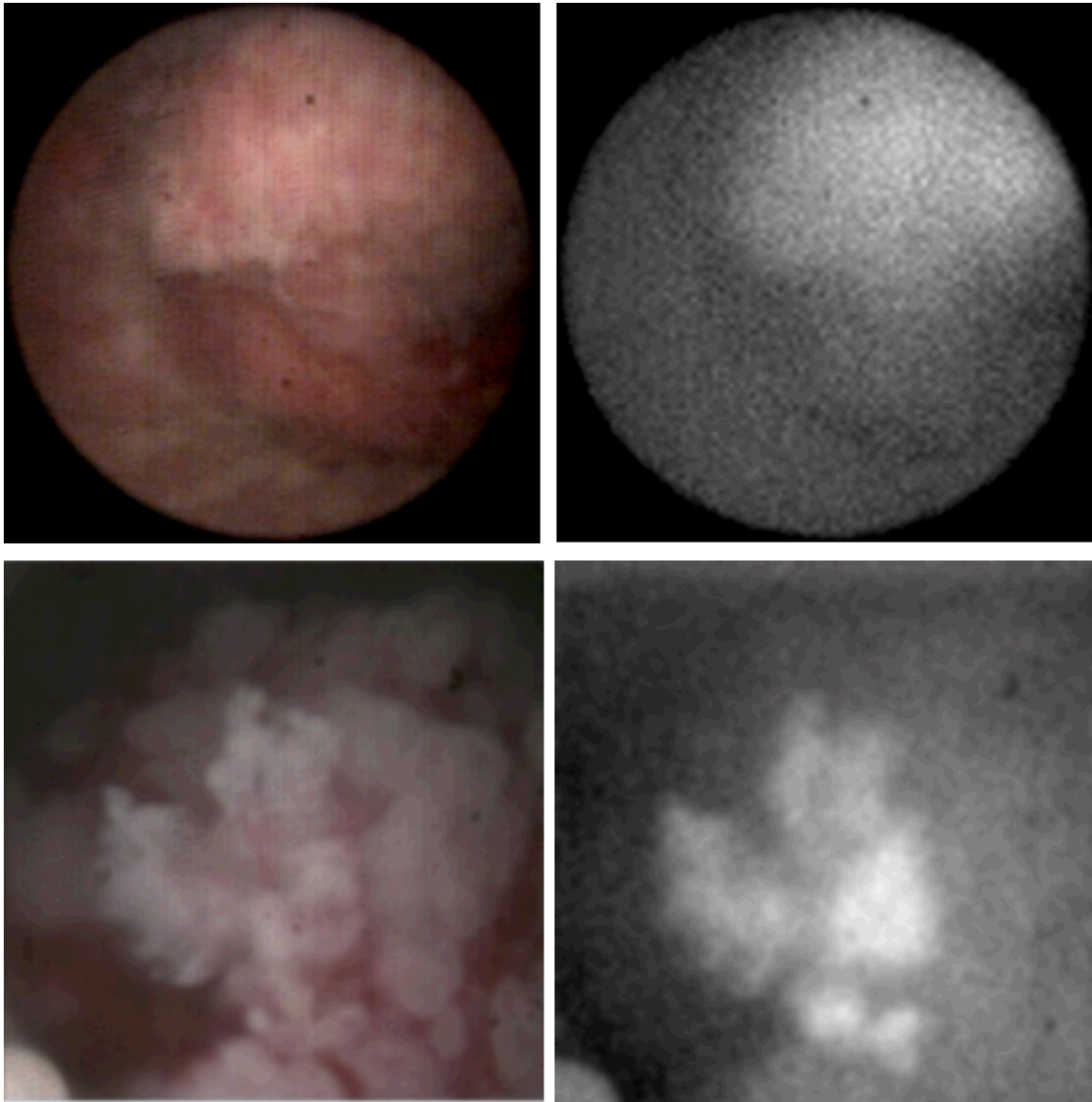


Figure 4: RGB and NIR images of tumors exhibiting a different amount of NIR autofluorescence at different locations. Top images: sessile high grade, muscle invasive bladder tumor. Bottom images: papillary high grade, T1 (invasive into lamina propria but not into underlying muscle) bladder tumor.

Images of more advanced tumors are shown in Figure 4. The RGB and NIR image pair shown on the top represent a sessile, high grade T2 (muscle invasive) tumor .

A characteristic observation in this case is that the NIR autofluorescence intensity arising from different part of the tumor significantly varies. Specifically, the upper part of the tumor provides a stronger autofluorescence signal than the lower part of the tumor. This part also appears as a less colored (whiter) feature in the RGB image. A similar effect is observed in the bottom image pair which shows a papillary, high grade T1 tumor at a closer range. A well-defined structure clearly identifiable in the RGB image provides a much stronger signal in the NIR autofluorescence image.

This was a relatively common observation during our preliminary *in vivo* experiment where certain parts of more advanced tumors exhibit a stronger signal than the rest of the tumor or that of the normal tissue. We hypothesize that this may arise from the presence of necrotic tissue in more advanced tumors and possible the presence of calcifications as we have observed in our *ex vivo* studies. However, in many cases the signal was moderately higher than normal tissue or the rest of the tumor such as in the case shown in figure 4 (top image pair). It is unclear whether this observation is clinically valuable. However, we do not exclude the possibility that some more advanced tumors have increased concentration of porphyrins (or other type of NIR fluorescence producing biomolecule), which give rise to NIR autofluorescence as is discussed in more detail in the next section.

Figure 5 shows the RGB and corresponding NIR AF images after a previous resection of a high grade T1 tumor months prior. The perimeter of the lesion appeared as a very bright object similar to tumor with necrotic tissue. The pathology from this lesion was reactive urothelium and necrosis; visually, it was the necrotic component (the lighter colored areas) that gave rise to the visually different in strength (increased) NIR autofluorescence signal.

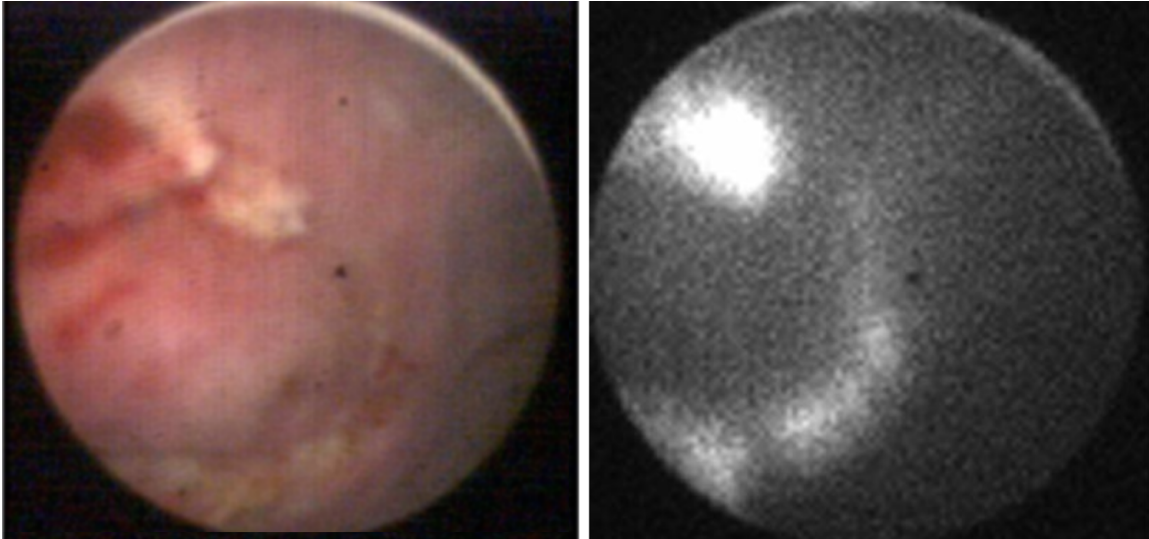


Figure 5. RGB and NIR images of reactive urothelium with focal areas of necrosis.

Increased fluorescence was also observed after cauterization of tissue, which occurs typically during endoscopic surgery for removal of bladder tumors. A high electrical current is used to cut through the tissue and then at a lower current to cauterize areas of bleeding and to ablate cancer cells. This effect is exemplified in Figure 6. The cauterized area is visible in the RGB image from the brownish appearance of the tissue. The corresponding NIR AF image exhibits increased emission compared to the normal tissue. This suggests that this imaging method may be useful only before the last step of the treatment via cauterization and possibly other types of thermal ablation (e.g. radiofrequency ablation).

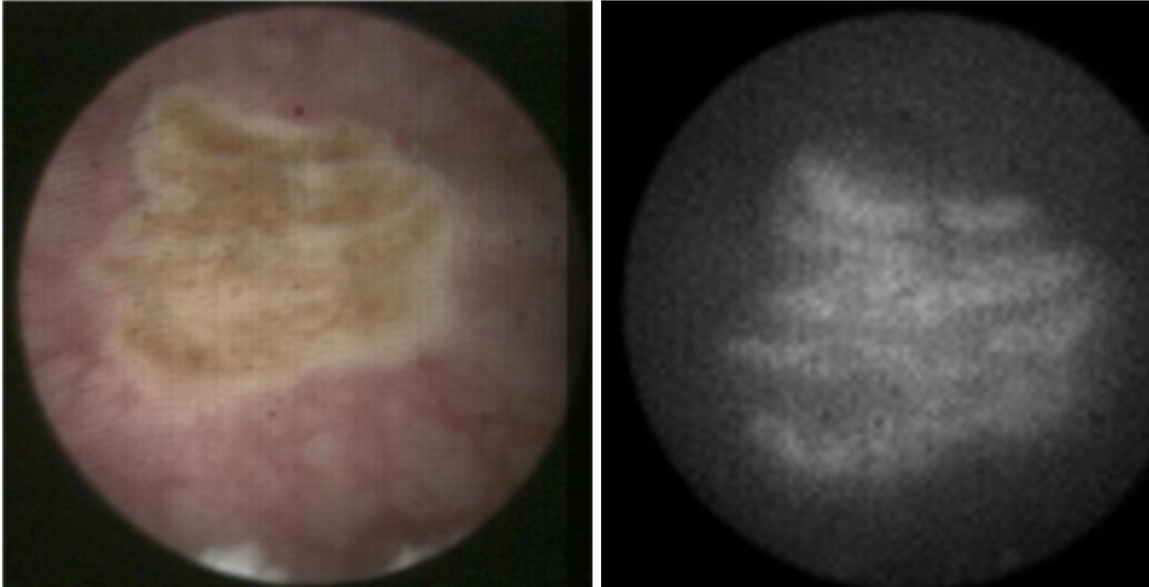


Figure 6. RGB and NIR images of a cauterized area of bladder urothelium illustrating artifact.

### *Discussion*

The observed NIR AF signal arises predominantly from the 650 nm laser excitation and is observed at a much lower level when the laser is turned off (when the excitation arises from the white light only). The system in its current form is not suitable for quantification of the recorded signal because there is no normalization to the excitation intensity. This is particularly important as different parts of the image are typically at different distances from the tip of the cystoscope and therefore, they receive different amounts of photo-excitation. In addition, tumors often have a papillary form but may also appear as sessile growths, which can lead to increased excitation compared to surrounding normal tissue during *in vivo* measurements. One simple way to approximate normalization of the NIR autofluorescence image would be to record the corresponding

light scattering image of the laser excitation, which would be a relatively simple addition to the current system.

The most important technical objective of this preliminary study was to explore whether this instrumentation design is capable of providing simultaneous and independent acquisition of the conventional RGB with the NIR AF images. The benefit of this instrumentation design is that the visual examination, which still remains the most important diagnostic method during surgery, is complemented by the spectral image(s) in the most efficient manner that allows for easy co-registration and correlation of image features and minimized acquisition time. It is also well recognized that the NIR autofluorescence intensity is very weak compared to that of visible autofluorescence arising from excitation in the UV or near UV spectral range. This necessitates the use of longer exposure times for image acquisition. Our prototype design allows these long exposure times for the acquisition of the NIR autofluorescence images (2 frames per second) without interfering with the acquisition of the standard video cystoscopy RGB images which are acquired at a standard video rate. The experimental results demonstrate that this technical objective was achieved as illustrated by figures 2-6. The images were displayed on separate monitors and the operator could easily correlate the spatial location of the features of interest in real time. Although the image quality was somewhat lower due to its transmission through the image preserving fiber bundle, this is a minor technical issue that can be addressed in future applications using a fiber bundle with larger number of fibers with a smaller core diameter. Complemented with use of imaging software, this minor issue can be effectively eliminated, at least at the level of the visual perception of the operator.

A significant reduction of the power of the white light illumination transmitted through the cystoscope was the result of the passing this light through the illumination assembly for spectral filtering. However, this did not limit acquisition of RGB images at 15 frames per second using a relatively inexpensive CCD camera. One frame per second was saved in the PC, which was used to also operate the CCD camera acquiring the NIR image. This limitation was imposed by the computer's processing speed, which was operating at its limit under the image acquisition and storage parameters used. The NIR autofluorescence images were acquired and saved at rate of 2 frames per second, which was a compromise to achieve a reasonable image quality that would allow features of interest to be clearly observable. As cystoscopes have a very narrow lens at the tip (small numerical aperture), it is challenging to implement an imaging method that is based on a weak signal such as the NIR AF component. Using a higher power laser would proportionally increase the detected NIR signal.

One of the most common problems of *in vivo* fluorescence imaging is the appearance of artifacts arising from heme in blood, which absorbs very strongly in the visible part of the spectrum. We hypothesized that excitation with a far red light (650 nm) would mitigate this problem. Our results, exemplified in figure 2, illustrate that the NIR fluorescence images acquired with this setup are relatively unaffected by the presence of blood.

While the technology described here is applicable to any type of endoscopy, the case of cystoscopic examination of bladder cancer is particularly illustrative of the need for development of additional visualization tools. 75% of patients with bladder cancer present with superficial disease (non-muscle-invasive, and confined to the mucosa—T<sub>a</sub> or

lamina propria—T<sub>1</sub>). While less than 20% of superficial bladder cancers progress to muscle-invasive disease (T<sub>2</sub>), about 50% of T<sub>a</sub> tumors and 70% of T<sub>1</sub> tumors will recur[11]. It has been shown that the recurrence rate of tumors with similar characteristics can vary substantially when compared by treatment institution[12], suggesting that completeness of initial resection may play a significant role in determining the fate of disease. Furthermore, it has become routine standard of care to bring patients with T<sub>1</sub> bladder tumors back to the operating room for re-resection because approximately 30% will show muscle-invasive disease on pathology from the second surgery[13], also probably reflecting a common tendency for incomplete initial resection of T<sub>1</sub> tumors. In addition, carcinoma *in situ* (CIS), a high grade, flat, superficial bladder lesion that carries a 20% of spreading into the upper tracts of the genitourinary system (into the ureters and/or kidneys) can easily be missed by white light cystoscopy because it often looks the same as bladder inflammation.

Among the novel types of imaging that have been developed to address these problems to date, the most successful has been fluorescent imaging involving either intravenous or topical application of 5-aminolevulinic acid (5-ALA) or its ester derivative, hexylester hexaminolevulinate (HAL) which has increased uptake into fatty (i.e. tumor) tissue than ALA. Synthesis of ALA occurs naturally in many tissues and is the rate limiting step in the production of heme. Exogenous ALA or HAL provided in large excess cause bioaccumulation of protoporphyrin IX (PpIX), the last molecular precursor to heme prior to enzymatic addition of iron by ferroketolase. PpIX is a potent fluorophore when excited by blue light (380-480 nm) and causes tumors to fluoresce more than normal tissue with red emission in the 625-725 nm region. This method has

been studied in several large series, including prospective, multicenter, randomized trials in Europe[14-17]. The largest of these studies showed that fluorescence diagnosis (FD) resulted in a nearly 20% increase in presence of residual tumors following initial resection and statistically significant increases in recurrence free survival up to eight years after the initial TURBT. Despite the successful outcomes associated with this technique, it has not gained widespread use, particularly outside of Europe. Reasons for this include a strong photobleaching effect [14] after about 30 minutes of fluorescence time[18, 19], the side effect of increased photosensitivity and possibly neurotoxicity when ALA is used systemically in concentrations that allow detectable tumor fluorescence[20]. In addition, the limited depth of penetration of the UV or visible blue excitation light used decreases its usefulness for deeper lesions, but most importantly a lack of specificity for cancer detection (37% false positive detection for HAL vs 26% for WLC[17]. Inflammation is the major source of false positive fluorescence[21]. Topical HAL is currently approved for use in Europe in the diagnosis of bladder cancer, and remains under consideration in the U.S. for FDA approval.

Compared to using ALA or HAL, the method we describe in this paper to detect bladder tumors has several potential advantages. First, the use of long wavelength (red) excitation light minimizes the absorption of heme which can lead to image artifacts, while still allowing detection of a near infrared fluorescence signal without necessarily using an exogenous fluorophore. Interestingly, the NIR is considered to be part of the spectrum in which there is relatively *little* native tissue absorption and autofluorescence, which has helped generate a large interest in developing dyes that fluoresce in the NIR for biological imaging [22]. The ability for the system we describe here to qualitatively

generate a NIR fluorescent signal that corresponds with presence of visible tumor reflects the high sensitivity that this combination of excitation and fluorescence wavelengths allow, without the loss of signal that would typically be associated by absorption of excitation light by heme.

The detection and imaging of cancer using administration of ALA or HAL discussed above can also be implemented using the current instrumentation maybe with only a minor modification on the laser wavelength to operate at 630 nm. This is because, although PpIX exhibits its maximum absorption in the blue and near UV spectral region, it also exhibits absorption extending to about 650 nm. With the ultrasensitive detection system used in this work, the emission from PpIX would be detected using concentrations that are multiple orders of magnitude lower to those used previously. This in turn means that much smaller concentration of ALA or HAL can be used that will help alleviate some of the issues of that method.

The instrumentation design presented in this work could be interfaced with NIR contrast agents that bind selectively to TCC (e.g. via an antibody-antigen interaction). This technological combination would theoretically increase the sensitivity and specificity of the method. Such NIR contrast agents are in the process of being developed [22].

The convenience of not needing to switch imaging modes during surgery increases the potential utility of including fluorescence imaging as a surgical tool in a way that has not yet been realized and increases the flexibility of the instrument to use in a wide variety of endoscopic applications. In addition, the use of relatively long wavelength excitation light increases the probe depth compared to what is possible using

UV or blue light for fluorophore excitation. The anticipated advantage is the ability to “see” tumor that is more extensive than superficial lesions that have so far been studied using fluorescence methods in endoscopy.

The finding of variations in NIR AF intensity in neoplastic bladder tissue with some tumors exhibiting higher AF than normal tissue is consistent with our previous experience with more advanced bladder tumor specimens studied *in vitro* (see figs. 1 and 2 in ref .9). In these ex-vivo studies, the images of more advanced tumors were from cross sectioned specimens following bladder resection. The higher NIR AF intensity regions were typically observed in the superficial layer of the tumors. The in vivo images obtained in this study represent a different viewing perspective (top view of the bladder surface as opposed to a cross section of the bladder tissue). We presumed that these areas that exhibited strong fluorescence were necrotic tissue and it seems likely that devitalized tissue undergoes a chemical change that increases its NIR AF properties. In addition, as discussed above, there is an increased porphyrin production in the bladder tumor in response to an external stimulus (ALA administration). It has been shown before in various reports that tumors originating in various part of the body exhibit increased porphyrin content which would probably increase the NIR fluorescence signal. This effect has been shown in one of our previous reports using ex vivo specimens. It is possible that bladder tumors at some stage of their development may start exhibiting this behavior. Additional experiments will be needed to elucidate the cause for the variation in behavior we see for different tumors. We also do not yet have a set of experiments that included patients with possible carcinoma *in situ* (CIS), so it is unclear how these lesions would exhibit NIR AF compared to normal tissue.

The most important limitation of the device we describe here given its current configuration, is the fluorescence artifact seen in cauterized and necrotic tissue. The images seen in Figure 3 confirm the presence of a higher fluorescence signal from even mild cautery compared with the normal tissue. The reasons for these high artifactual signals are not yet clear, since to our knowledge there have never been similar images presented in the literature. While this phenomenon should be studied further in a clinical environment, ultimately the best application for this technology may be use in a non-surgical setting (e.g. in an ambulatory clinic environment) prior to use of cautery.

### *Conclusion*

A novel instrument which utilizes long wavelength visible excitation and near-infrared fluorescence in combination with conventional white light endoscopy has been developed. The images we present here suggest high qualitative sensitivity given that tissue autofluorescence in the NIR part of the spectrum occurs typically at low amplitude. Cancer tumors were qualitatively visible with NIR autofluorescence *in vivo*. Necrotic, calcified, and cauterized tissue exhibited artifactual increased NIR autofluorescence.

### *Acknowledgements*

This research is supported by funding from Lawrence Livermore National Laboratory and the Center for Biophotonics, an NSF Science and Technology Center, managed by the University of California, Davis, under Cooperative Agreement No. PHY 0120999. This work was performed in part under the auspices of the U.S. Department of Energy by Lawrence Livermore National Laboratory under Contract DE-AC52-07NA27344.

## References

1. Moghissi, K., M.R. Stringer, and K. Dixon, *Fluorescence photodiagnosis in clinical practice*. Photodiagnosis Photodyn Ther, 2008. **5**(4): p. 235-7.
2. Wagnieres, G.A., W.M. Star, and B.C. Wilson, *In vivo fluorescence spectroscopy and imaging for oncological applications*. Photochem Photobiol, 1998. **68**(5): p. 603-32.
3. Ramsoekh, D., J. Haringsma, J.W. Poley, P. van Putten, H. van Dekken, E.W. Steyerberg, M.E. van Leerdam, and E.J. Kuipers, *A back-to-back comparison of white light video endoscopy with autofluorescence endoscopy for adenoma detection in high-risk subjects*. Gut, 2010. **59**(6): p. 785-93.
4. Banerjee, A.K., P.H. Rabbitts, and J. George, *Lung cancer . 3: Fluorescence bronchoscopy: clinical dilemmas and research opportunities*. Thorax, 2003. **58**(3): p. 266-71.
5. Lam, S., C. MacAulay, J.C. leRiche, and B. Palcic, *Detection and localization of early lung cancer by fluorescence bronchoscopy*. Cancer, 2000. **89**(11 Suppl): p. 2468-73.
6. Richards-Kortum, R. and E. Sevick-Muraca, *Quantitative optical spectroscopy for tissue diagnosis*. Annu Rev Phys Chem, 1996. **47**: p. 555-606.
7. Kalyanasundaram, K., *Photochemistry of polypyridine and porphyrin complexes*. 1992, London ; San Diego: Academic Press. 626 p.
8. Zawirski, B., *Comparative porphyrin content in tumors with contiguous non-neoplastic tissues*. Neoplasia, 1979. **26**(2): p. 223-9.
9. Demos, S.G., R. Gandour-Edwards, R. Ramsamooj, and R. deVere White, *Spectroscopic detection of bladder cancer using near-infrared imaging techniques*. J Biomed Opt, 2004. **9**(4): p. 767-71.
10. Demos, S.G., R. Gandour-Edwards, R. Ramsamooj, and R. White, *Near-infrared autofluorescence imaging for detection of cancer*. J Biomed Opt, 2004. **9**(3): p. 587-92.
11. Kiemeneij, L.A., J.A. Witjes, R.P. Heijbroek, F.M. Debruyne, and A.L. Verbeek, *Dysplasia in normal-looking urothelium increases the risk of tumour progression in primary superficial bladder cancer*. Eur J Cancer, 1994. **30A**(11): p. 1621-5.
12. Brausi, M., L. Collette, K. Kurth, A.P. van der Meijden, W. Oosterlinck, J.A. Witjes, D. Newling, C. Bouffieux, and R.J. Sylvester, *Variability in the recurrence rate at first follow-up cystoscopy after TUR in stage Ta T1 transitional cell carcinoma of the bladder: a combined analysis of seven EORTC studies*. Eur Urol, 2002. **41**(5): p. 523-31.
13. Schwaibold, H.E., S. Sivalingam, F. May, and R. Hartung, *The value of a second transurethral resection for T1 bladder cancer*. BJU Int, 2006. **97**(6): p. 1199-201.
14. Denzinger, S., M. Burger, B. Walter, R. Knuechel, W. Roessler, W.F. Wieland, and T. Filbeck, *Clinically relevant reduction in risk of recurrence of superficial bladder cancer using 5-aminolevulinic acid-induced fluorescence diagnosis: 8-year results of prospective randomized study*. Urology, 2007. **69**(4): p. 675-9.
15. Grossman, H.B., L. Gomella, Y. Fradet, A. Morales, J. Presti, C. Ritenour, U. Nseyo, and M.J. Droller, *A phase III, multicenter comparison of hexaminolevulinic acid fluorescence cystoscopy and white light cystoscopy for the*

- detection of superficial papillary lesions in patients with bladder cancer.* J Urol, 2007. **178**(1): p. 62-7.
16. Jichlinski, P., L. Guillou, S.J. Karlsen, P.U. Malmstrom, D. Jocham, B. Brennhovd, E. Johansson, T. Gartner, N. Lange, H. van den Bergh, and H.J. Leisinger, *Hexyl aminolevulinate fluorescence cystoscopy: new diagnostic tool for photodiagnosis of superficial bladder cancer--a multicenter study.* J Urol, 2003. **170**(1): p. 226-9.
  17. Jocham, D., F. Witjes, S. Wagner, B. Zeylemaker, J. van Moorselaar, M.O. Grimm, R. Muschter, G. Popken, F. Konig, R. Knuchel, and K.H. Kurth, *Improved detection and treatment of bladder cancer using hexaminolevulinate imaging: a prospective, phase III multicenter study.* J Urol, 2005. **174**(3): p. 862-6; discussion 866.
  18. Steinbach, P., H. Weingandt, R. Baumgartner, M. Kriegmair, F. Hofstadter, and R. Knuchel, *Cellular fluorescence of the endogenous photosensitizer protoporphyrin IX following exposure to 5-aminolevulinic acid.* Photochem Photobiol, 1995. **62**(5): p. 887-95.
  19. Robinson, D.J., H.S. de Bruijn, N. van der Veen, M.R. Stringer, S.B. Brown, and W.M. Star, *Fluorescence photobleaching of ALA-induced protoporphyrin IX during photodynamic therapy of normal hairless mouse skin: the effect of light dose and irradiance and the resulting biological effect.* Photochem Photobiol, 1998. **67**(1): p. 140-9.
  20. Peng, Q., T. Warloe, K. Berg, J. Moan, M. Kongshaug, K.E. Giercksky, and J.M. Nesland, *5-Aminolevulinic acid-based photodynamic therapy. Clinical research and future challenges.* Cancer, 1997. **79**(12): p. 2282-308.
  21. Zaak, D., M. Kriegmair, H. Stepp, R. Baumgartner, R. Oberneder, P. Schneede, S. Corvin, D. Frimberger, R. Knuchel, and A. Hofstetter, *Endoscopic detection of transitional cell carcinoma with 5-aminolevulinic acid: results of 1012 fluorescence endoscopies.* Urology, 2001. **57**(4): p. 690-4.
  22. Escobedo, J.O., O. Rusin, S. Lim, and R.M. Strongin, *NIR dyes for bioimaging applications.* Curr Opin Chem Biol, 2010. **14**(1): p. 64-70.